Article

Safety Analysis of Grounding Resistance with Depth of Water for Floating PVs

Jae Woo Ko [1], Hae Lim Cha [1], David Kwang-Soon Kim [1], Jong Rok Lim [1], Gyu Gwang Kim [1], Byeong Gwan Bhang [1], Chang Sub Won [2], Han Sang Jung [3], Dong Hyung Kang [4] and Hyung Keun Ahn [1],*

[1]   Department of Electrical Engineering, Konkuk University, 120 Neungdong-ro, Gwangjin-gu, Seoul 05029, Korea; zeusko@naver.com (J.W.K.); haelim219@gmail.com (H.L.C.); davidkskim0324@gmail.com (D.K.-S.K.); bangsil82@hanmail.net (J.R.L.); rbrhkd00@naver.com (G.G.K.); bbk0627@naver.com (B.G.B.)

[2]   Power Conversion R&D Center, LS IS Co., Ltd., LS-ro 116 beon-gil 40, Dongan-gu, Anyang-si 14118, Gyeonggi-do, Korea; cswon@lsis.com

[3]   Water Facility Research Center, K-Water Institute (KWI), 125, 1689 beon-gil, Yuseong-daero, Yuseong-gu, Daejeon 34045, Korea; han-sang@kwater.or.kr

[4]   Operation & Management Team, K-Water Institute (KWI), K-Water Hapcheon Dam Office, 705, Hapcheonhosu-ro, Yongju-myeon, Hapcheon-gun 50215, Gyeongsangnam-do, Korea; kowa1995@kwater.or.kr

*   Correspondence: hkahn@konkuk.ac.kr; Tel.: +82-2-450-3481

Abstract: Underwater grounding methods could be applied in deep water for grounding a floating PV (photovoltaic) system. However, the depth at which the electrodes should be located is a controversial subject. In this study, grounding resistance was measured for the first time by analyzing the water temperature at different water depths in an area where a floating PV system is installed. The theoretical calculation of the grounding resistance has a maximum error range of 8% compared to the experimentally measured data. In order to meet the electrical safety standards of a floating PV system, a number of electrodes were connected in parallel. In addition, the distance between electrodes and number of electrodes were considered in the test to obtain a formula for the grounding resistance. In addition, the coefficient of corrosion was obtained from an electrode installed underwater a year ago, and it was added to the formula. Through this analysis, it is possible to predict the grounding resistance prior to installing the floating PV system. Furthermore, the electrical safety of the floating PV system could be achieved by considering the seasonal changes in water temperature.

Keywords: floating PV system; grounding resistance; electrical safety; underwater grounding

1. Introduction

Photovoltaic (PV) systems have become one of the major sustainable energy resources as a practical solution to environmental problems. The energy generated by PV systems have played an important role over the last decade in the evolution of the electricity field, offering a unique opportunity for the growth of mixed production of electricity on a large scale [1–3]. The energy produced by PV systems in Europe, which currently amounts to 4% of the peak demand on the continent (with 51 GW installed), could reach a maximum of 25% of European demand in 2030, contributing significantly to the reduction of greenhouse gas emissions and decreasing use of fossil fuels [4,5]. When a PV system is installed in structures on land, there are critical issues such as choosing the location, ensuring structural safety, and considering the interference of shadows. In addition, it is necessary to address

public concerns as well as resolve potential licensing issues for installations in areas such as farmlands or forests. Therefore, a floating PV system on a water surface has been recently suggested as an alternative [6]. The floating PV is a new concept and is not at the commercial stage at present. Only some demonstrator projects are currently being installed worldwide [7]. In a floating PV system, the PV module is installed and operated in humid areas (on bodies of water or in wetlands) and the electricity produced is transmitted to the power grid for end users. The installation of the system is understandably more difficult compared with land-based PV systems; however, the power generation efficiency of a floating PV system is 10–15% higher than that of a land-based PV system because of the ambient temperature drop, which is caused by the absorption of the evaporation heat and reflection of light from the water surface [8–12]. There is also a positive effect on the proliferation of green algae [13]. In Australia, it was reported that 40% of the water in a reservoir could be lost through evaporation [14]. A floating PV system could prevent this phenomenon and manage water resources more efficiently. Despite the rapid increase in the number of PV power stations, their safe grounding system design is rarely analyzed in the literature [15]. A grounding system must be installed to prevent possible damage by lightning or current leakage. Furthermore, it allows for the flow of normal or fault currents into the earth without exceeding operating and equipment limits or affecting service continuity in an adverse manner [16]. Any form of physical contact made with improperly grounded lightning currents could be extremely dangerous to human life. The steep rise in lighting current within microseconds, coupled with the inductance of the object it strikes, could generate step or touch potentials with values well above the safety limit that the human body can endure. Lightning has been acknowledged as a primary source of power quality degradation in power systems [17]. There have been an enormous amount of studies conducted on various aspects of the grounding system, with the most recent ones as found in the literature [18–21]. The specifications for the safe design of a PV system are currently defined by International Standards: NEC (National Electrical Code) 2011 [22] and UL (Underwriters Laboratories Inc.) 1741 for the countries of North America [23]. Lightning and surge protection is the main issue of the standard IEC (International Electrotechnical Commission) 62305 (parts 1 to 4). Each part provides basic criteria for the protection of structures and services, risk management methods, lightning protection system (LPS), and protection against lightning electromagnetic impulse (LEMP), respectively [24–27]. It is common knowledge that the grounding resistance should be less than approximately 10 Ω, as required by the electrical utility laws. Unfortunately, grounding methods for floating PV systems are not clearly established yet. Under these circumstances, there have been some experimental studies concerning grounding safety in a floating PV system [28]. It is possible to draw grounding cables to the surface in a shallow reservoir or lake and hook them up in the same manner as performed in land-based PV systems. It would be very inefficient to install the grounding cable on land outside a deep lake or dam. This paper presents an underwater grounding method that uses the water resistivity instead of earth resistivity to calculate the theoretical resistance, which was predicted and validated by measuring the grounding resistance and temperature variations associated with water depth.

2. Calculation of Grounding Resistance

2.1. Measurement of Grounding Resistance

The fall-of-potential method is widely used to measure grounding resistance. E is the electrode to be measured, and C is the electrode used to apply a current, as shown in Figure 1. P is the electrode used to measure the potential difference at E. The power source is connected between E and C, and the current is passed through the earth to obtain the potential difference between E and P. When the current I (A) flows to the earth, the potential difference between E and P is V (V). The grounding resistance is then obtained, assuming that P and C are at equal potentials.
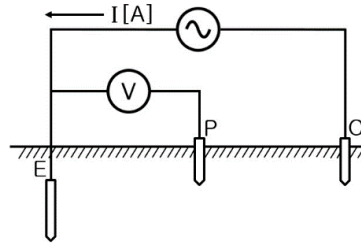
Figure 1. Fall-of-potential method.

2.2. Equivalent Resistance of Multilayer Resistance

The most practical measurements of the earth's resistivity utilize a formula that assumes that the earth is made of homogeneous layers. However, in the case of non-homogeneous layers, the resistivity of each layer should be substituted with the equivalent resistivity.

The equivalent resistivity ρ_0 can be calculated assuming that the resistivity of each layer is connected in parallel with ρ_1, ρ_2, ρ_3 ..., as shown in Figure 2a:

$$\frac{h_1 + h_2 + h_3}{\rho_0} = \frac{h_1}{\rho_1} + \frac{h_2}{\rho_2} + \frac{h_3}{\rho_3} + \frac{\infty}{\rho_4}. \tag{1}$$

When the driven rod is grounded to the earth as shown in Figure 2b, the equivalent resistivity (ρ_m) can be expressed as given in Equation (2):

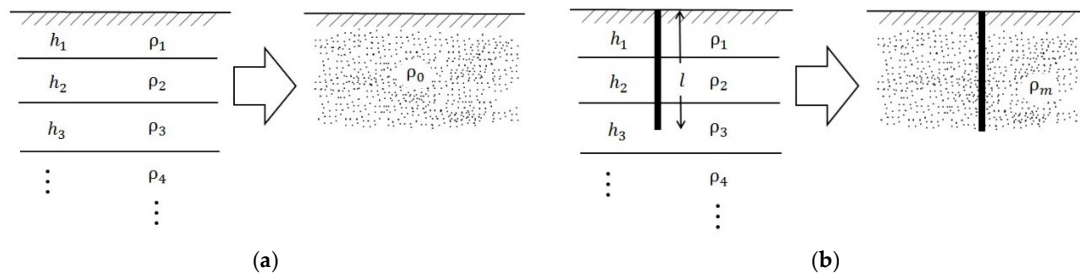$$\rho_m = \frac{l}{\frac{h_1}{\rho_1} + \frac{h_2}{\rho_2} + \frac{l - (h_1 + h_2)}{\rho_3}}. \tag{2}$$

Figure 2. Equivalent resistivity of a multilayer. (**a**) Without driven rod; (**b**) with driven rod.

3. Modeling of Multilayer Resistance According to Water Temperature

3.1. Measurement of Water Temperature According to Water Depth

The water resistivity is divided into zones in deep water. The different resistivity of each layer results from the variation in water temperature with depth. This experiment was conducted at the Hapcheon Dam, located in the southern part of the Korean peninsula. The dam is used to control floods and consists of 790 km^3 of pondage, and has a total area of 925 km^2 and an average water depth of over 30 m. The variations in water temperature with depth were measured at every 1 m from 1 m to 30 m below the surface. The monthly averages were then calculated from the daily data to compare and analyze the seasonal variations.

It is known that the water temperature decreases as we go deeper below the surface of the water, as shown in Figure 3a–c. Figure 3a shows the variations in water temperature in spring and fall, respectively. Figure 3b,c indicate the variations in water temperature in the summer and winter, respectively. In the summer, there is a considerable difference of more than 20 °C between the

temperatures at the surface and 30 m below the surface, as shown in Figure 3b. Therefore, a difference in resistivity between layers is expected. On the other hand, there is little difference in the water temperature with changing water depth in the winter. Accordingly, no major difference in resistivity would be found between the layers. Figure 3d shows a graph of the monthly average air temperature and the highest and the lowest water temperature for each month. The highest water temperature recorded tends to be greater than the average air temperature. It also shows that the difference between the highest and the lowest water temperatures is smallest in the winter (January) while it is the largest in the summer (August) reaching around 22 °C. It is therefore expected that the resistivity of water will show huge differences at the surface of water and in deeper water.

According to observations made over a period of one year, the temperature of the water dropped during the winter, began to rise steadily in the spring, and reached a maximum in the summer, before gradually decreasing throughout the fall and winter. The water temperature at approximately 30 m below the surface shows little difference over the year.
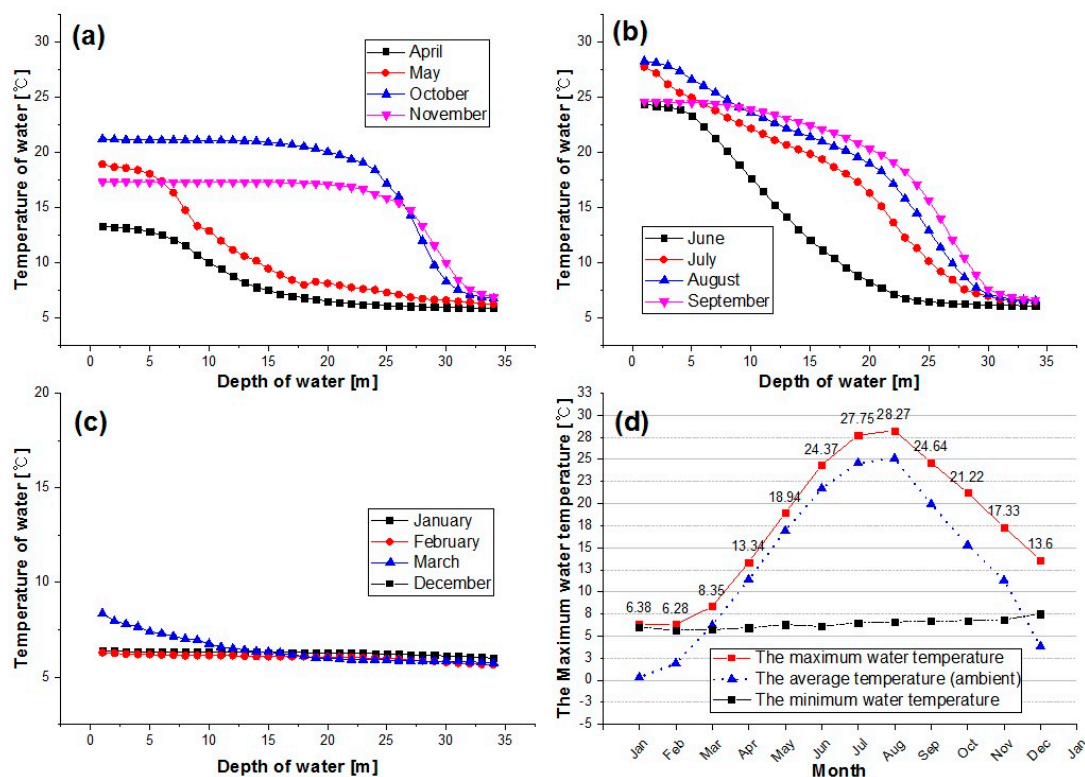

Figure 3. Seasonal water temperature against water depth at Hapcheon Dam (**a**) in spring and fall; (**b**) in summer; (**c**) in winter; and (**d**) monthly water temperature and average temperature.

3.2. Experiment on Water Resistivity According to Temperature

Generally, the resistivity of materials tends to increase as the temperature increases. The electrical resistivity was corrected for the soil temperature and referenced to 25 °C, as shown in Equation (3) [29]:

$$\frac{1}{\rho_T} = \sigma_T = \sigma_{25}[1 + \alpha(T - 25\ °C)], \tag{3}$$

where ρ_T is the electrical resistivity at temperature T (in °C), σ_T is the electrical conductivity at T, $\sigma_{25\,°C}$ is the electrical conductivity at 25 °C, and α is the correction factor per °C accounting for the linear increase in soil conductivity with temperature. Water samples were taken from places such as rivers, reservoirs, and the Hapcheon Dam, where a floating PV system could be installed in order to

measure the water resistivity according to the variations in water temperature. The water samples were set in a thermo-hygrostat and the resistivity was measured by controlling the external temperature. A conductivity meter was also used for measurements at every 5 °C for the whole range of 5–30 °C, as well as for resistivity measurements required to reduce errors.

The experimental results in Figure 4 illustrate that the resistivity of water ranged from 15–35 Ω·m with a reference temperature of 25 °C, and tended to increase with decreasing temperature.
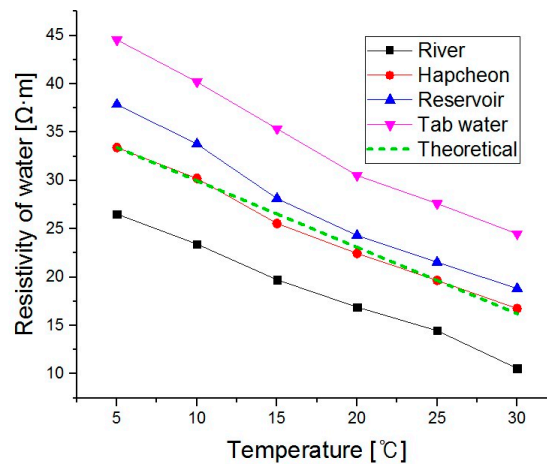

Figure 4. Resistivity of water from various sources against temperature.

The results obtained from the experiment were remarkably consistent with the theoretical value calculated from Equation (3), with 0.39% error. The temperature coefficient calculated based on the above experiment was used for modeling the grounding resistivity.

3.3. Modeling Grounding Resistivity for a Floating PV System According to a Multilayer Structure

The underwater grounding for a floating PV system must be installed at a specific water depth, in contrast to a land-based PV system, as shown in Figure 5. In this case, the system can be divided into three main sections: the first section between the surface and top of the electrode, the second section including the electrode, and the third section between the bottom of the electrode and the bottom of the water body. Each section has a different resistivity; therefore, a different formula should be used to calculate the total equivalent resistivity instead of the existing formula.
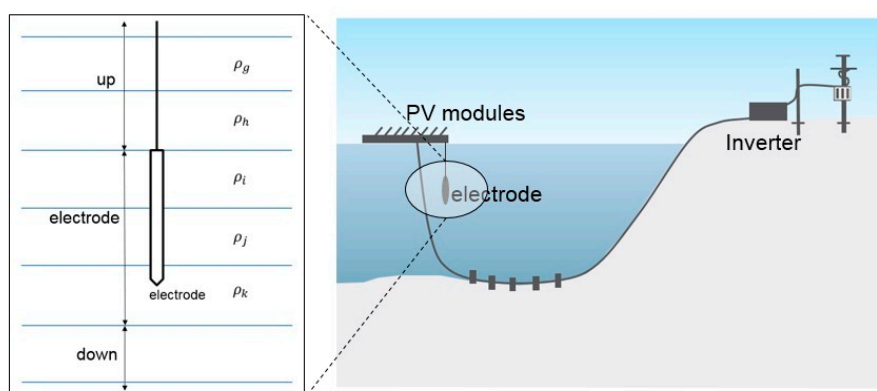

Figure 5. Design for an underwater grounding system for a floating PV (Photovoltaic) system.

The resistivity for the section above the electrode (ρ_{up}) of length l (m) located between sections i and k in a multilayer structure can be obtained with

$$\rho_{up} = \frac{\sum_{x=1}^{i-1} h_x}{\sum_{x=1}^{i-1} \frac{h_x}{\rho_x}}, \tag{4}$$

where h_x is the distance between the layers and ρ_x represents the resistivity of the layers. On the other hand, the resistivity of water for the section including the electrode with length l (m) is given by

$$\rho_{electrode} = \frac{l}{\sum_{x=i}^{k-1} \frac{h_x}{\rho_x} + \frac{l-\sum_{x=i}^{k-1} h_x}{\rho_k}}. \tag{5}$$

Finally, the resistivity of the water for the section between the bottom of electrode and the bottom of the water body can be expressed as (A = water depth)

$$\rho_{down} = \frac{\sum_{x=k+1}^{A} h_x}{\sum_{x=k+1}^{A} \frac{h_x}{\rho_x}}. \tag{6}$$

Therefore, the total resistivity of the water is $\rho_{total} = \rho_{electrode} + \rho_{down}$, which can be calculated by adding Equations (4)–(6) as shown below:

$$\rho_{total} = \frac{\sum_{x=1}^{i-1} h_x}{\sum_{x=1}^{i-1} \frac{h_x}{\rho_x}} + \frac{l}{\sum_{i=1}^{k=1} \frac{h_x}{\rho_x} + \frac{l-\sum_{x=i}^{k-1} h_x}{\rho_k}} + \frac{\sum_{x=k+1}^{A} h_x}{\sum_{x=k+1}^{A} \frac{h_x}{\rho_x}}. \tag{7}$$

In conclusion, final grounding resistance in the floating PV system is shown in Equation (8) by substituting Equation (11) into basic grounding resistance equation:

$$R_{grounding\ resistance} = \frac{\left(\frac{\sum_{x=1}^{i-1} h_x}{\sum_{x=1}^{i-1} \frac{h_x}{\rho_x}} + \frac{l}{\sum_{i=1}^{k=1} \frac{h_x}{\rho_x} + \frac{l-\sum_{x=i}^{k-1} h_x}{\rho_k}} + \frac{\sum_{x=k+1}^{A} h_x}{\sum_{x=k+1}^{A} \frac{h_x}{\rho_x}} \right)}{2\pi l} ln\frac{4l}{d}. \tag{8}$$

If the sections are infinite, it is possible to analyze by integral. To use this method, variation of water temperature according to depth of water should be indicated as a formula.

4. Simulations and Experiments for the Measurement of Grounding Resistance

MATLAB simulations and measurements of grounding resistance in this study were conducted to validate the proposed equation. The resistivity of water was 19.66 $\Omega{\cdot}$m when the water temperature reached the reference temperature (25 °C) in the experiment. The distance between layers was set as 0.5 m considering the minimum length of the electrode.

The values shown in Table 1 were used to simulate Equation (8). An experiment was performed at the Hapcheon Dam in order to verify the results of this simulation. The grounding resistance was measured every 1 m by lowering the electrode until it reached the maximum depth of 30 m. A standard electrode was used for the simulation and an M-1000U was used to measure variations in the temperature of the water at different depths. Grounding resistance was measured by the KEW 4106 (Kyoritsu), which has 0.1 Ω of resolution and $\pm$2%rdg of accuracy. The prime parameters in this study are the water temperature and the consequent variations in water resistivity. Therefore, in order to obtain accurate results, the electrode was located at the measuring depth for 5 min as a stabilizing time until the temperature of the electrode was the same as that of the water.

Table 1. Simulation parameters for the grounding resistance.

Parameter		Value	
Resistivity of water 25 °C		19.66 Ω·m	
Length of electrode	0.5 m	1 m	1.8 m
Diameter of electrode	12 mm	14 mm	16 mm
Distance between the layer		0.5 m	
Depth of water		40 m	

5. Considerations for the Design of a Grounding System for Floating PV Systems

Unlike land-based PV systems, there are three important considerations for the design of a grounding system for floating PV systems: (1) the coefficient of parallel connection; (2) corrosion of electrodes; and (3) coefficient of seasonal variation. These factors should be considered in case the grounding system is installed underwater.

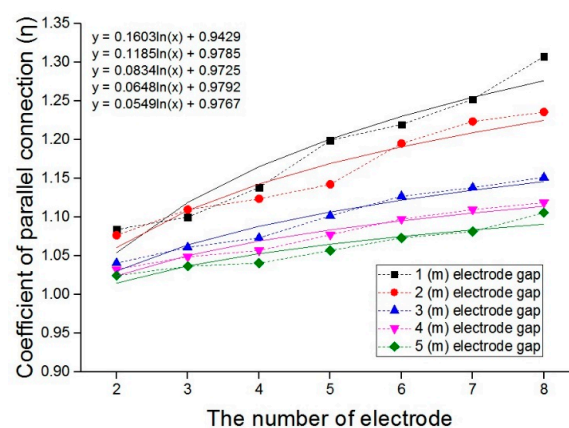### 5.1. Coefficient of Parallel Connection

In general, the electrodes are connected in parallel to obtain a grounding resistance that meets standards. For instance, in the case where two electrodes with grounding resistance R (Ω) are connected in parallel, the equivalent resistance would be $R/2$ (Ω) ideally. However, in reality, the coefficient of parallel connection is added, as shown in Equation (9):

$$R_0 = \eta \frac{R}{Z}. \tag{9}$$

R is one grounding resistance and Z is the number of electrodes and η is the coefficient of parallel connection. The coefficient of parallel connection has been determined experimentally and can be applied to a floating PV system.

Figure 6 shows the coefficient of parallel connection for grounding resistance, which was calculated by changing the number of electrodes and the distance between electrodes. Based on the five equations in Figure 6, the final calculated coefficient of parallel connection is given by Equation (10):

$$\eta_f = [-06068 \ln(l) + 0.1613] \ln(Z) + 0.0068l + 0.9495. \tag{10}$$

Figure 6. Coefficient of parallel connection vs. the number of electrodes (floating PV system).

5.2. Coefficient of Corrosion

There should be corrosion on the electrodes installed underwater for long periods and it increases the grounding resistance. To confirm the tendency of increasing grounding resistance, electrodes have

been installed in the dam and reservoir for a year. Measurements were carried out once every three months, and the results are indicated in Figure 7 after temperature correction. In order to see difference by environment clearly, temperature condition was adjusted equally in this paper even though two installing areas have similar temperature.
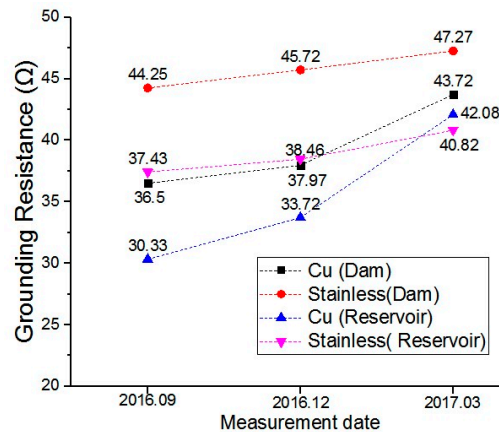

Figure 7. Grounding resistances of floating PV systems at the dam and reservoir (temperature corrected).

Based on the measured values above, theoretically calculated coefficients of corrosion are given in Table 2; coefficients of corrosion for the dam and reservoir are marked separately since these places have different installation environments.

Table 2. Coefficients of corrosion.

	Coefficient of Corrosion (Ω/Month)	
	Cu	**Stainless**
Dam	1.20	0.50
Reservoir	0.74	0.57

5.3. Coefficient of Seasonal Variation

The resistivity of water varies remarkably for each season. This indicates that the grounding resistance depends on the depth at which the electrode is installed underwater. Figure 8 shows the variation in water temperature by water depth for a year.
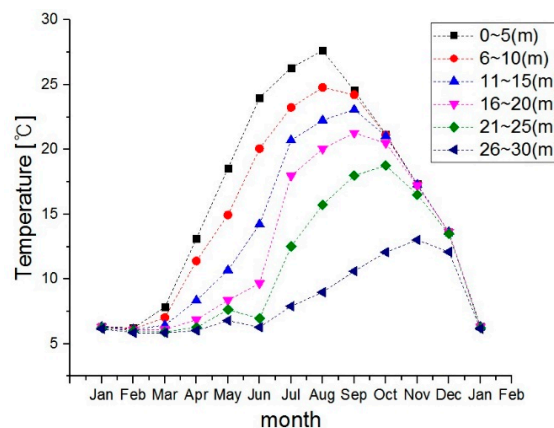

Figure 8. Monthly temperature changes by water depth.

The most significant change in temperature occurs on the water surface, which implies that the grounding resistance on the surface will undergo the largest change. The grounding resistance was calculated basis variation of water temperature as shown in Table 3.

Table 3. Coefficients of variation by season.

Depth of Water (m)	Maximum Difference of Water Temperature (°C)	Coefficient of Variation by Season (Ω)
1~5	23	15.513
6~10	19	12.815
11~15	17	11.466
16~20	15	10.117
21~25	12	8.094
26~30	7	4.721

6. Results and Discussion

Simulation results show that the grounding resistance of a 1.8 m length electrode is the smallest at 48.36 Ω. The shorter the length and diameter of the electrode, the higher the grounding resistance. The smaller surface area indicates that the amount of current required to discharge is relatively small. The deeper the burial depth, the greater the grounding resistance, as shown in Figure 9; this tendency is contrary to the distribution of the water temperature with respect to water depth. Figure 10 shows both the theoretically calculated values and practically measured values of the grounding resistance. The maximum errors between the theoretical and measured values were ±8.14, ±8.88, and ±6.45%, for electrodes with lengths of 0.5 m, 1 m, and 1.8 m, respectively. It was difficult to predict an accurate grounding resistance because water is a fluid.

Furthermore, Figure 9 shows that the error increases with decreasing electrode length because electrode resistance is less affected by the multilayer structure of water, which is a theoretical division made for predictions.
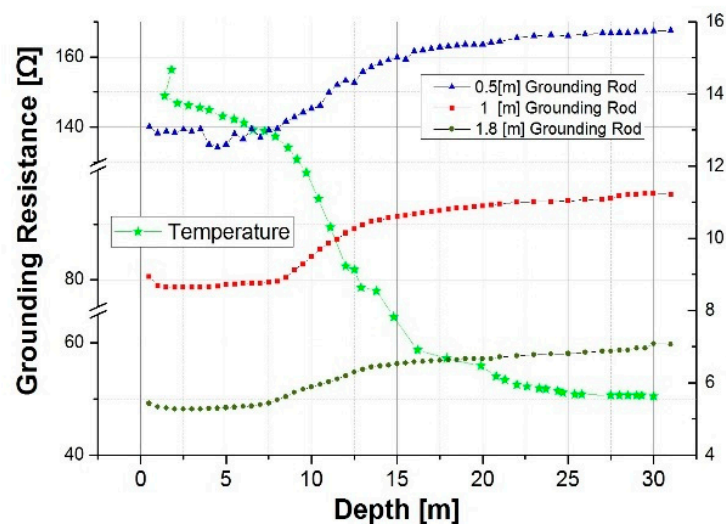

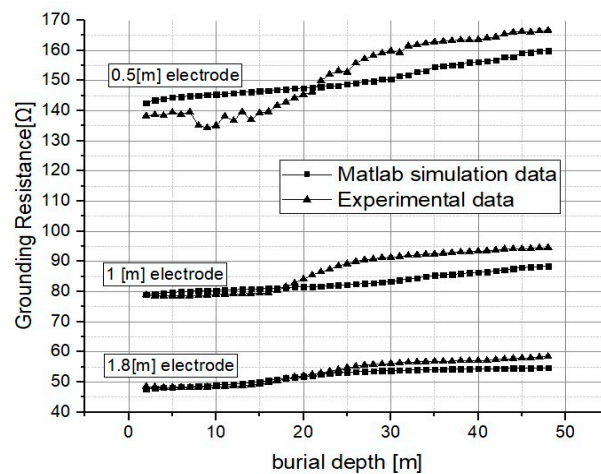**Figure 9.** Comparison between grounding resistance and water temperature.

Figure 10. Theoretical and measured values of grounding resistance.

In the case of a floating PV system, an additional coefficient should be applied to Equation (9) considering the aforementioned three factors as below in Equation (11):

$$R_0 = \eta_f(l, Z) \frac{R_G + \alpha(t)t}{Z} \beta.$$ (11)

Equation (11) contains coefficient $\alpha(t)$ and $\beta(t)$, which should be applied for floating PV system particularly. R_0, η, R, Z mean the total combined resistance, coefficient of parallel connection, grounding resistance for a single electrode, and the number of electrodes, respectively. $\alpha(t)$ indicates increasing grounding resistance over time. β is the coefficient of seasonal variation and it means the grounding resistance varies with season. Grounding resistance has been measured to verify Equation (11) at the Hapcheon dam, and the results are as shown in Figure 11.
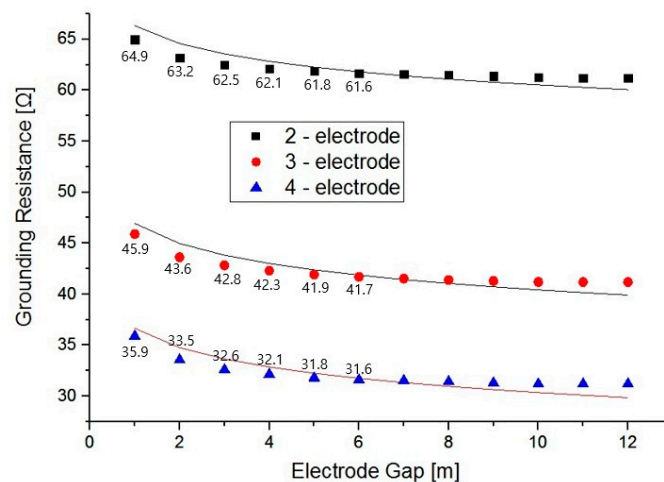

Figure 11. Comparison between grounding resistance and electrode gap.

The errors between theoretical values and the test results ranged from −1.13 to 1.38 Ω for two electrodes, −1.28 to 1.35 Ω for three electrodes, and −1.33 to 1.19 Ω for four electrodes, respectively. The average percentage error was 1.2% for two electrodes, 1.7% for three electrodes, and 2.3% for four electrodes, respectively. Figure 11 was calculated based on data of water resistivity as per depth of water in May 2017. R_g in Equation (8) constantly changes, so date of measurement should be indicated together with grounding resistance.

7. Conclusions

Grounding involves connecting a conductor to the earth to protect electric circuits or electric equipment. The grounding method for a floating PV system is slightly different from the grounding method for a PV system on land. This is because it is difficult to install a grounding system outside or at the bottom of a body of water where the floating PV system is located. Therefore, direct underwater grounding methods need to be considered for these systems. Such underwater grounding methods offer benefits in terms of cost; however, the grounding resistance is difficult to estimate. Therefore, the temperature of the water should be measured according to its depth in the area where the floating PV system is installed in order to predict the temperature-dependent resistivity of the water. Grounding resistance is then calculated by modeling the resistivity based on the position of the electrode in the water. The electrical safety of the floating PV system, which is critical in protecting it against environmental conditions, can be achieved throughout the grounding resistance design process and its verification.

Author Contributions: Jae Woo Ko developed his own primary model for the resistance with water environments especially focusing on the depth of water. Hae Lim Cha, David Kwang-soon Kim and Jong Rok Lim added experimental data analysis with different seasons. Gyu Gwang Kim and Byeong Gwan Bhang established experimental methods at 2 test sites by the technical supports from Han Sang Jung and Dong Hyung Kang with safety issues. Chang Sub Won and Hyung Keun Ahn integrated the resistance design from the respect of system level to guarantee the safety with times to provide reliable floating photovoltaic power station which would be one of key systems in near future for the micro-grid network.

Conflicts of Interest: The authors declare no conflict of interest.

References

1. Biagi, M.; Falvo, M.C. Smart Micro Grid Programming for RES: From Communication to Dispatching. In Proceedings of the IET Renewable Power Generation Conference (RPG 2014), Naples, Italy, 24–25 September 2014.
2. Brenna, M.; Falvo, M.C.; Foiadelli, F.; Martirano, L.; Poli, D. Sustainable energy microsystem (SEM): Preliminary energy analysis. In Proceedings of the International Conference on Smart Grid Technologies (IEEE ISGT), Washington, DC, USA, 16–20 January 2012.
3. Capparella, S.; Falvo, M.C. Secure faults detection for preventing fire risk in PV systems. In Proceedings of the International Carnahan Conference on Security Technology (IEEE ICCST), Rome, Italy, 13–16 October 2014.
4. European Photovoltaic Industry Association (EPIA). *Connecting the Sun, Solar Photovoltaics on the Road to Large-Scale Grid Integration*; EPIA: Brussels, Belgium, 2012.
5. European Photovoltaic Industry Association (EPIA). *Global Market Outlook for Photovoltaics until 2016*; EPIA: Brussels, Belgium, 2012.
6. Trapani, K.; Millar, D.L. Proposing offshore photovoltaic (PV) technology to the energy mix of the Maltese islands. *Energy Convers. Manag.* **2012**, *67*, 18–26. [CrossRef]
7. Trapani, K.; Millar, D.L.; Smith, H.C.M. Novel offshore application of photovoltaics in comparison to conventional marine renewable energy technologies. *Renew. Energy* **2013**, *50*, 879–888. [CrossRef]
8. Ferrer-Gisbert, C.; Ferrán-Gozálvez, J.J.; Redón-Santafé, M.; Ferrer-Gisbert, P.; Sánchez-Romero, F.J.; Torregrosa-Soler, J.B. A new photovoltaic floating cover system for water reservoirs. *Renew. Energy* **2013**, *60*, 63–70. [CrossRef]
9. Bahaidarah, H.; Subhan, A.; Gandhidasan, P.; Rehman, S. Performance evaluation of a PV (photovoltaic) module by back surface water cooling for hot climatic conditions. *Energy* **2013**, *59*, 445–453. [CrossRef]
10. Choi, Y.K. A Study on Power Generation Analysis of Floating PV System Considering Environmental Impact. *Int. J. Softw. Eng. Its Appl.* **2014**, *8*, 75–84. [CrossRef]
11. Abdolzadeh, M.; Ameri, M. Improving the effectiveness of a photovoltaic water pumping system by spraying water over the front of photovoltaic cells. *Renew. Energy* **2009**, *34*, 91–96. [CrossRef]

12. Radziemska, E. The effect of temperature on the power drop in crystalline silicon solar cells. *Renew. Energy* **2003**, *28*, 1–12. [CrossRef]

13. Alam, M.Z.B.; Ohgaki, S. Evaluation of UV-radiation and its residual effect for algal growth control. In *Advances in Water and Wastewater Treatment Technology*, 1st ed.; Matsuo, T., Hanaki, K., Satoh, H., Eds.; Elsevier: Amsterdam, The Netherlands, 2001; pp. 109–117.

14. Helfer, F.; Lemckert, C.; Zhang, H. Impacts of climate change on temperature and evaporation from a large reservoir in Australia. *J. Hydrol.* **2012**, *475*, 365–378. [CrossRef]

15. Ma, J.; Dawalibi, F.P. Grounding analysis of a solar power generation facility. In Proceedings of the 2010 Asia-Pacific Power and Energy Engineering Conference, Chengdu, China, 28–31 March 2010.

16. Institute of Electrical and Electronics Engineers (IEEE). IEEE Guide for Safety in AC Substation Grounding. IEEE Std 80-2000. 15 May 2015. Available online: http://ieeexplore.ieee.org/document/7109078/ (accessed on 27 July 2017).

17. Saini, M.K.; Kapoor, R. Classification of power quality events—A review. *Int. J. Electr. Power Energy Syst.* **2012**, *43*, 11–19. [CrossRef]

18. Mohamad Nor, N.; Trlep, M.; Abdullah, S.; Rajab, R. Investigations of earthing systems under steady-state and transients with FEM and experimental work. *Int. J. Electr. Power Energy Syst.* **2013**, *44*, 758–763. [CrossRef]

19. Mohamad Nor, N.; Abdullah, S.; Rajab, R.; Othman, Z. Comparison between utility sub-station and imitative earthing systems when subjected under lightning response. *Int. J. Electr. Power Energy Syst.* **2012**, *43*, 156–161. [CrossRef]

20. Mohamad Nor, N.; Rajab, R.; Othman, Z. Validation of the earth resistance formulae using computational and experimental methods for gas insulated sub-station (GIS). *Int. J. Electr. Power Energy Syst.* **2012**, *43*, 290–294. [CrossRef]

21. Mohamad Nor, N.; Abdullah, S.; Rajab, R.; Ramar, K. Field tests: Performances of practical earthing systems under lightning impulses. *Int. J. Electr. Power Energy Syst.* **2013**, *45*, 223–228. [CrossRef]

22. National Fire Protection Association (NFPA). *National Electrical Code (NEC)*; NFPA: Quincy, MA, USA, 2011.

23. Underwriters Laboratories Inc. *UL1741 Standard, Inverters, Converters, Controllers and Interconnection System Equipment for Use with Distributed Energy Resources*; Underwriters Laboratories Inc.: Melville, NY, USA, 2010.

24. International Electrotechnical Commission (IEC). *IEC Std. 62305-1, Protection against Lightning—Part 1: General Principles*; IEC: London, UK, 2006.

25. International Electrotechnical Commission (IEC). *IEC Std. 62305-2, Protection against Lightning—Part 2: Risk Management*; IEC: London, UK, 2006.

26. International Electrotechnical Commission (IEC). *IEC Std. 62305-3, Protection against Lightning—Part 3: Physical Damage to Structures and Life Hazard*; IEC: London, UK, 2006.

27. International Electrotechnical Commission (IEC). *IEC Std. 62305-4, Protection against Lightning—Part 4: Electrical and Electronic Systems within Structures*; IEC: London, UK, 2006.

28. Choi, Y.K. An Experimental Study on Ground Resistivity and Grounding Resistance of Water Environment. *J. Korea Acad.-Ind. Coop. Soc.* **2014**, *15*, 2343–2348. [CrossRef]

29. Campbell, R.B.; Bower, C.A.; Richards, L.A. Change of electrical conductivity with temperature and the relation of osmotic pressure to electrical conductivity and ion concentration for soil extracts. *Soil Sci. Soc. Am. Proc.* **1948**, *13*, 66–69. [CrossRef]